

## **Electronic Supplementary Information**

### **Synthesis, Structural Characterization, and Multichannel Anion and Cation Sensing Studies of a Bifunctional Ru(II) Polypyridyl-Imidazole Based Receptor**

**Shyamal Das, Srikanta Karmakar, Sourav Mardanya, and Sujoy Baitalik<sup>\*a</sup>**

Department of Chemistry, Inorganic Chemistry Section, Jadavpur University,  
Kolkata 700032, India

**Table S1** Selected bond distances (Å) and bond angles (deg) for **1**

Bond distances(angstrom)	
Ru1-N1	2.079(5)
Ru1-N4	2.069(6)
Ru1-N8	2.044(6)
Ru1-N9	2.067(6)
Ru1-N10	2.037(6)
Ru1-N11	2.029(6)
Bond angles(degree)	
N1-Ru1-N4	78.8(2)
N1-Ru1-N8	173.8(3)
N1-Ru1-N9	95.5(2)
N1-Ru1-N10	87.6(2)
N1-Ru1-N11	95.5(2)
N4-Ru1-N8	99.3(2)
N4-Ru1-N9	83.4(2)
N4-Ru1-N10	96.8(2)
N4-Ru1-N11	172.9(2)
N8-Ru1-N9	78.4(3)
N8-Ru1-N10	98.5(2)
N8-Ru1-N11	86.9(2)
N9-Ru1-N10	176.8(2)
N9-Ru1-N11	101.5(2)
N10-Ru1-N11	78.6(2)

**Table S2** Spectrophotometric and fluorometric detection limit of **1** in MeCN and H<sub>2</sub>O

	Detection Limit / M		
		In MeCN	In H <sub>2</sub> O
Absorption			
	F <sup>-</sup>	$4.34 \times 10^{-9}$	
	AcO <sup>-</sup>	$1.03 \times 10^{-8}$	
	H <sub>2</sub> PO <sub>4</sub> <sup>-</sup>	$2.30 \times 10^{-6}$ $1.89 \times 10^{-5}$	
	Fe <sup>2+</sup>	$6.68 \times 10^{-9}$	$2.18 \times 10^{-7}$
Emission			
	F <sup>-</sup>	$8.19 \times 10^{-9}$	$4.75 \times 10^{-5}$
	AcO <sup>-</sup>	$1.19 \times 10^{-8}$	
	H <sub>2</sub> PO <sub>4</sub> <sup>-</sup>	$1.99 \times 10^{-6}$ $1.90 \times 10^{-5}$	
	Fe <sup>2+</sup>	$6.78 \times 10^{-9}$	$2.38 \times 10^{-7}$

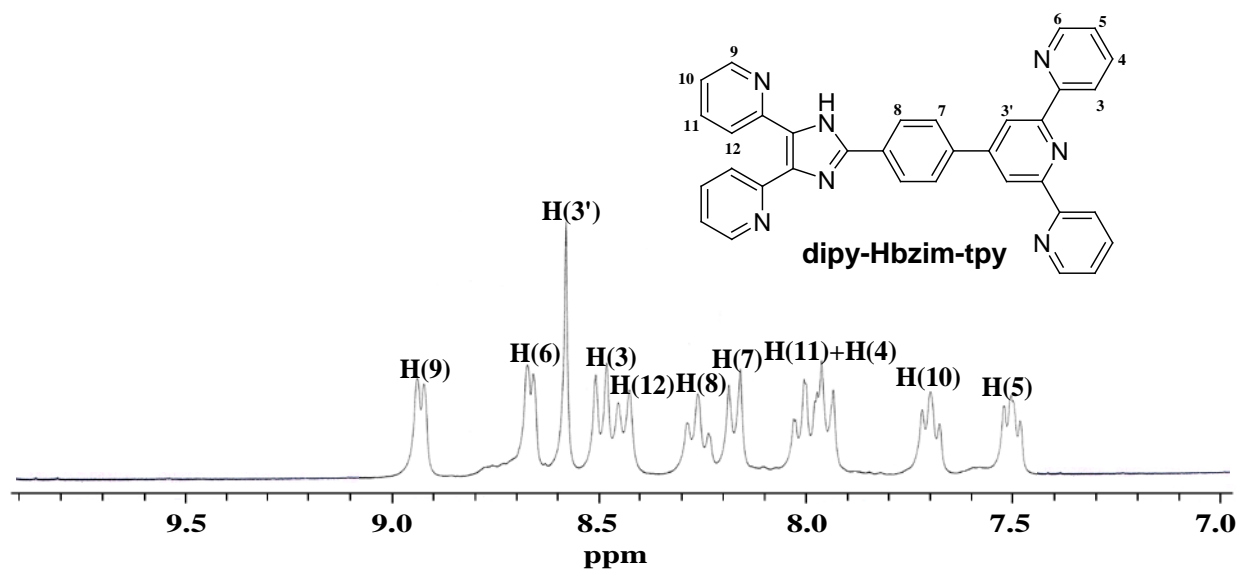


Fig. S1. <sup>1</sup>H NMR (300 MHz) spectrum of **dipy-Hbzim-tpy** in DMSO-*d*<sub>6</sub>.

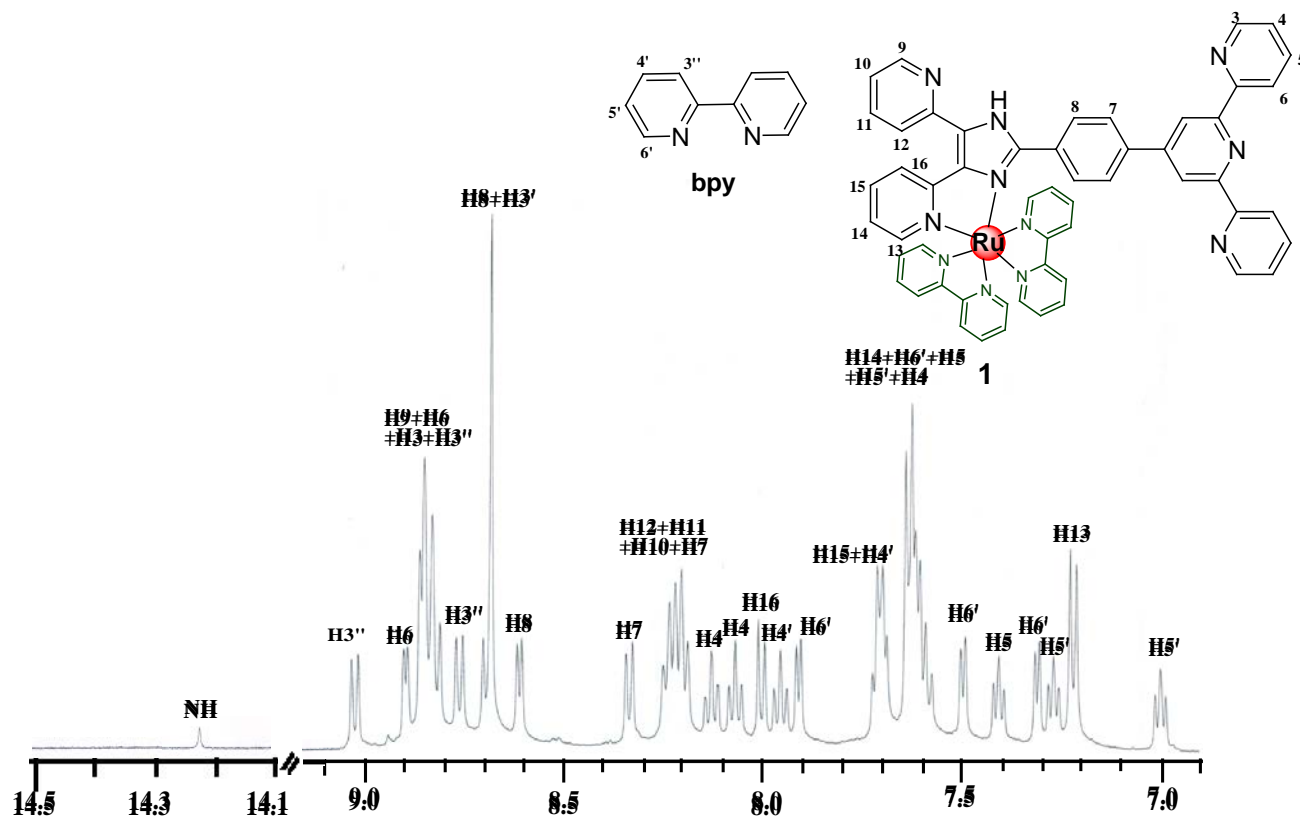
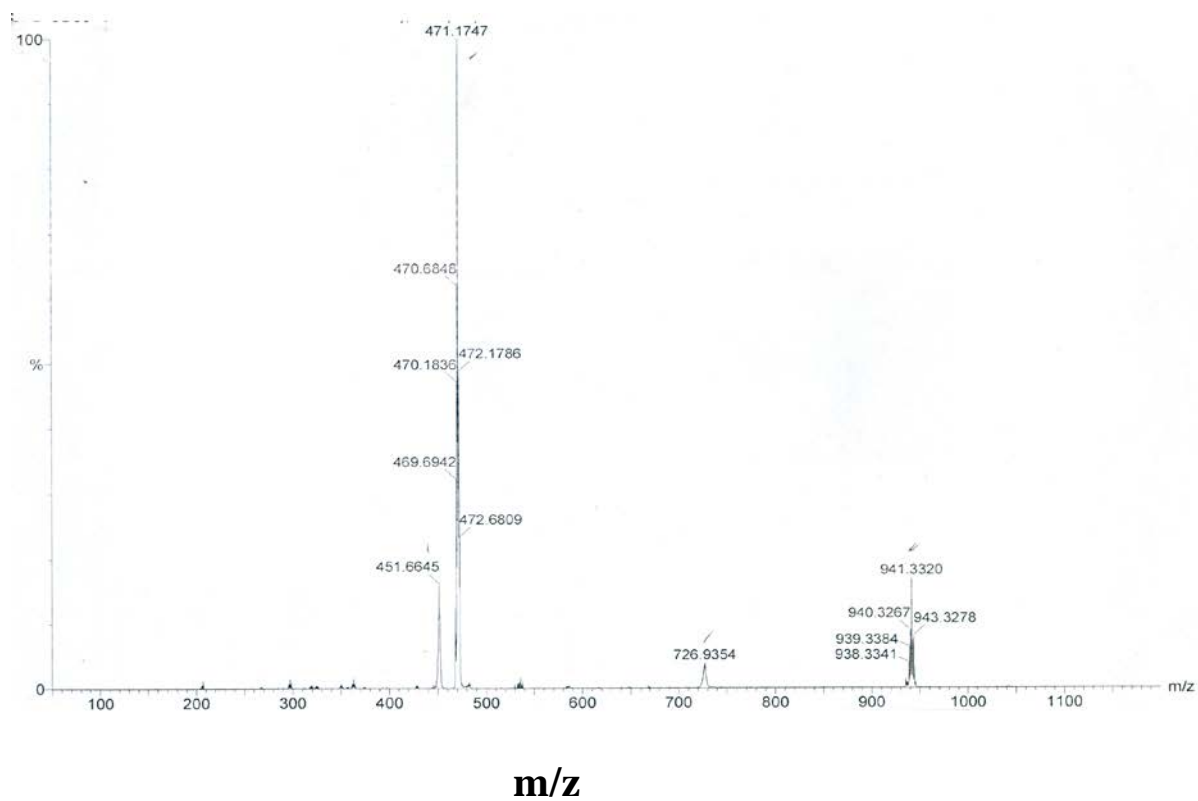
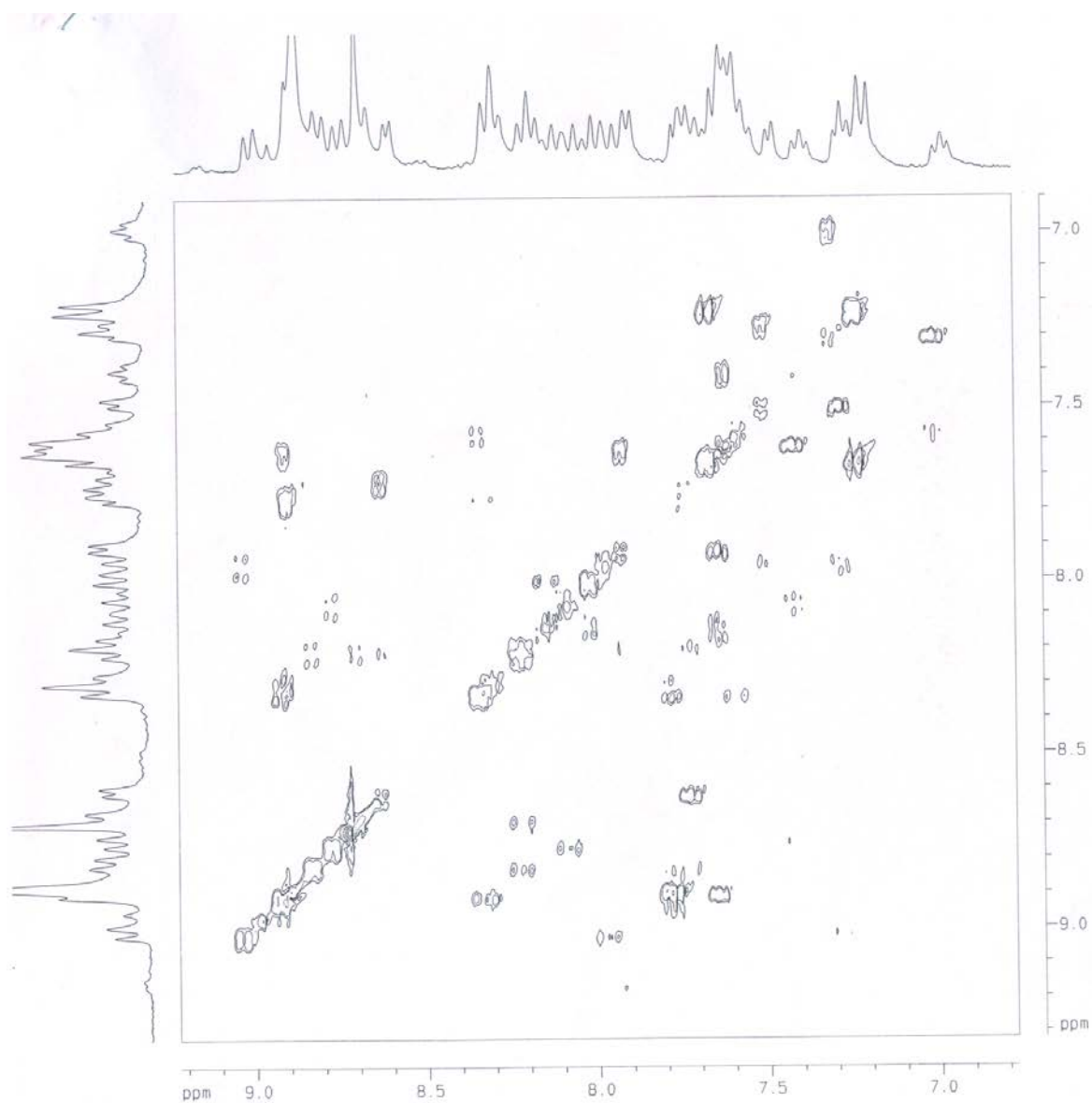


Fig. S2 <sup>1</sup>H NMR (500 MHz) spectrum of **1** in DMSO-*d*<sub>6</sub>.



**Fig. S3** Experimental ESI mass spectrum of **1** in acetonitrile.



**Fig. S4**  $^1\text{H}$ - $^1\text{H}$  COSY spectrum of **1**  $\text{DMSO-}d_6$ .

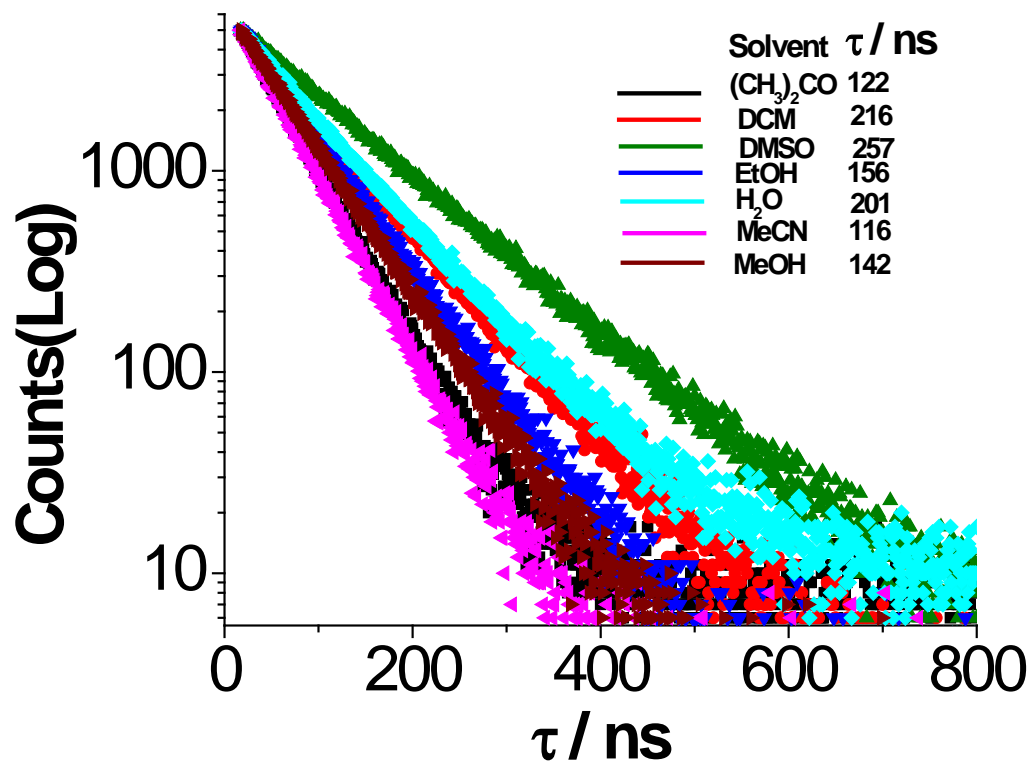


**Fig. S5** Time-resolved luminescence decay profiles of **1** at room temperature in different solvents. Lifetimes of **1** in different solvents are given in the inset of the figure.

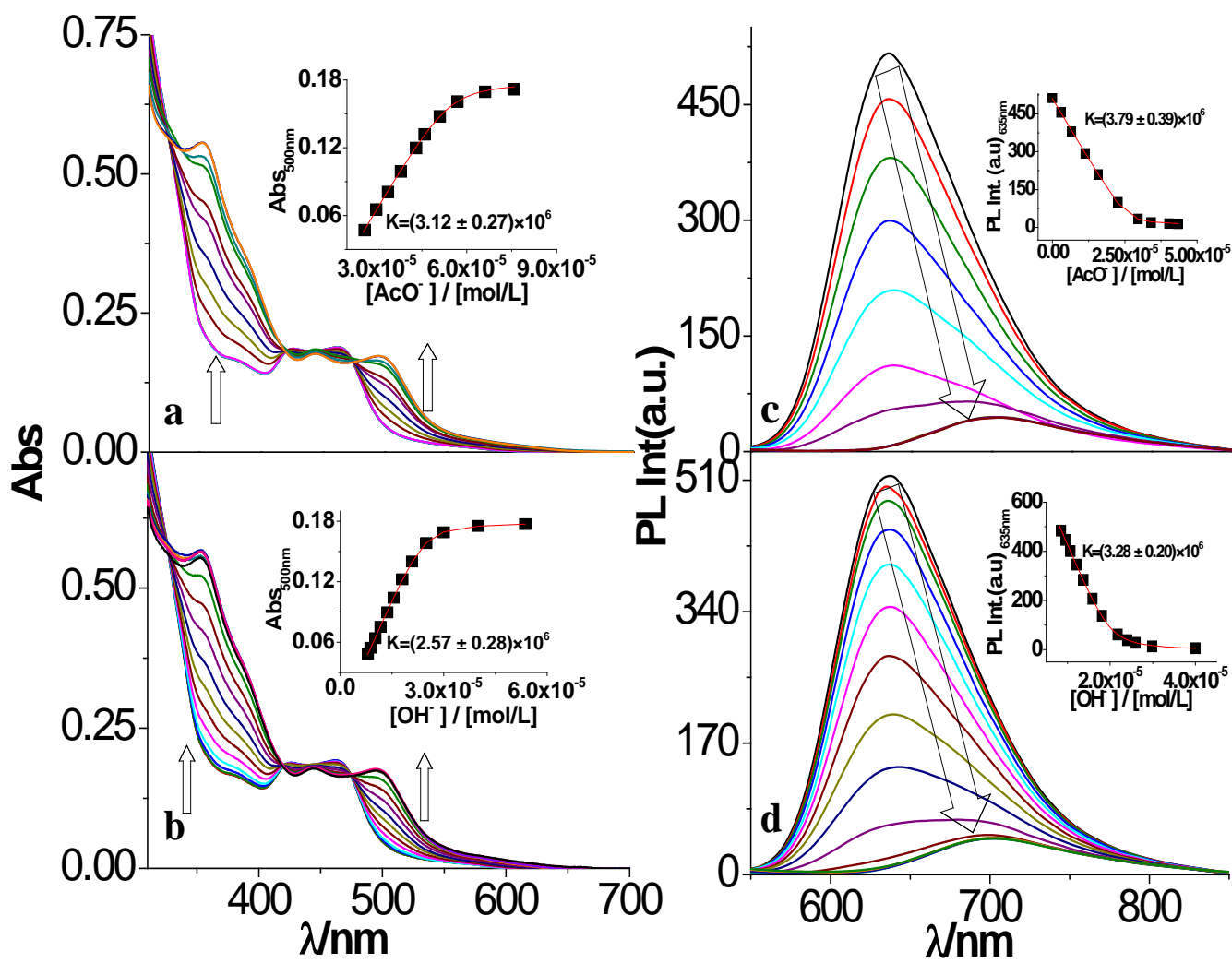


**Fig. S6** Changes in UV-vis absorption and photoluminescence spectra of **1** in acetonitrile upon addition of  $\text{AcO}^-$  (a and c, respectively) and  $\text{OH}^-$  (b and d, respectively) ions.

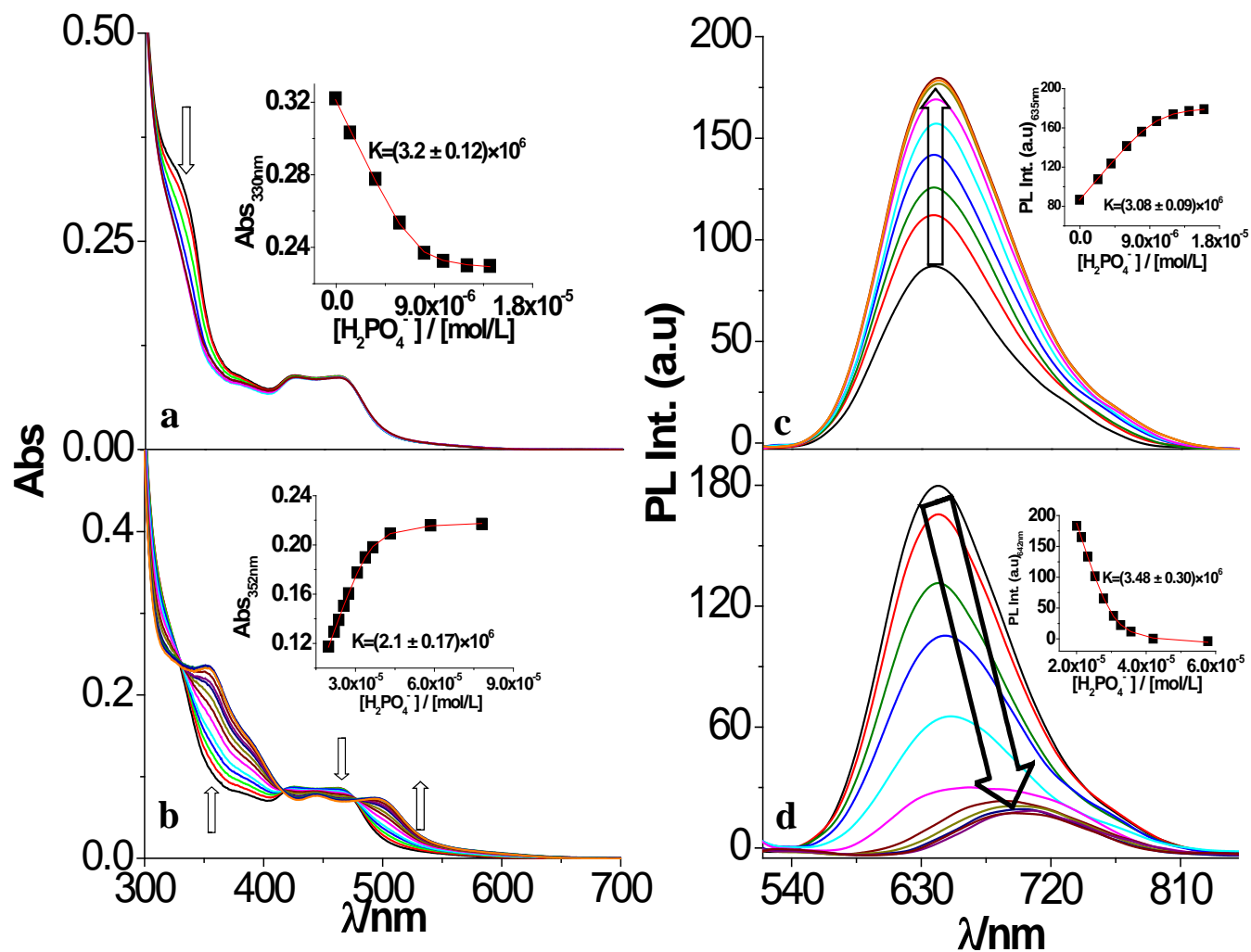


**Fig. S7** Changes in UV-vis absorption (a and b) and photoluminescence (c and d) spectra of **1** in acetonitrile upon incremental addition of  $\text{H}_2\text{PO}_4^-$ .

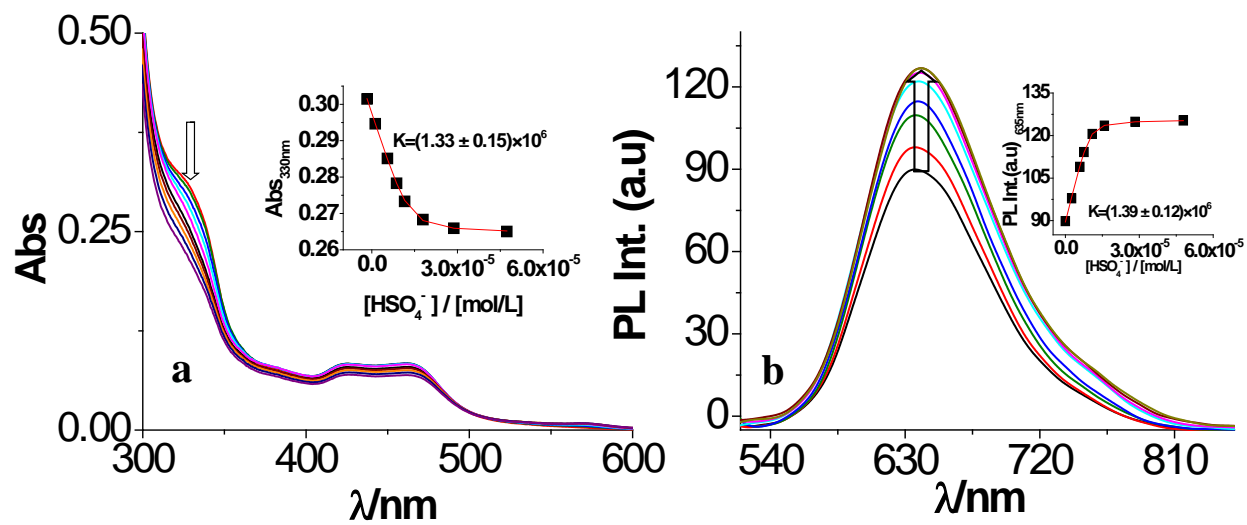


**Fig. S8** Changes in UV-vis absorption (a) and photoluminescence (b) spectra of **1** in acetonitrile upon addition of  $\text{HSO}_4^-$  ion.

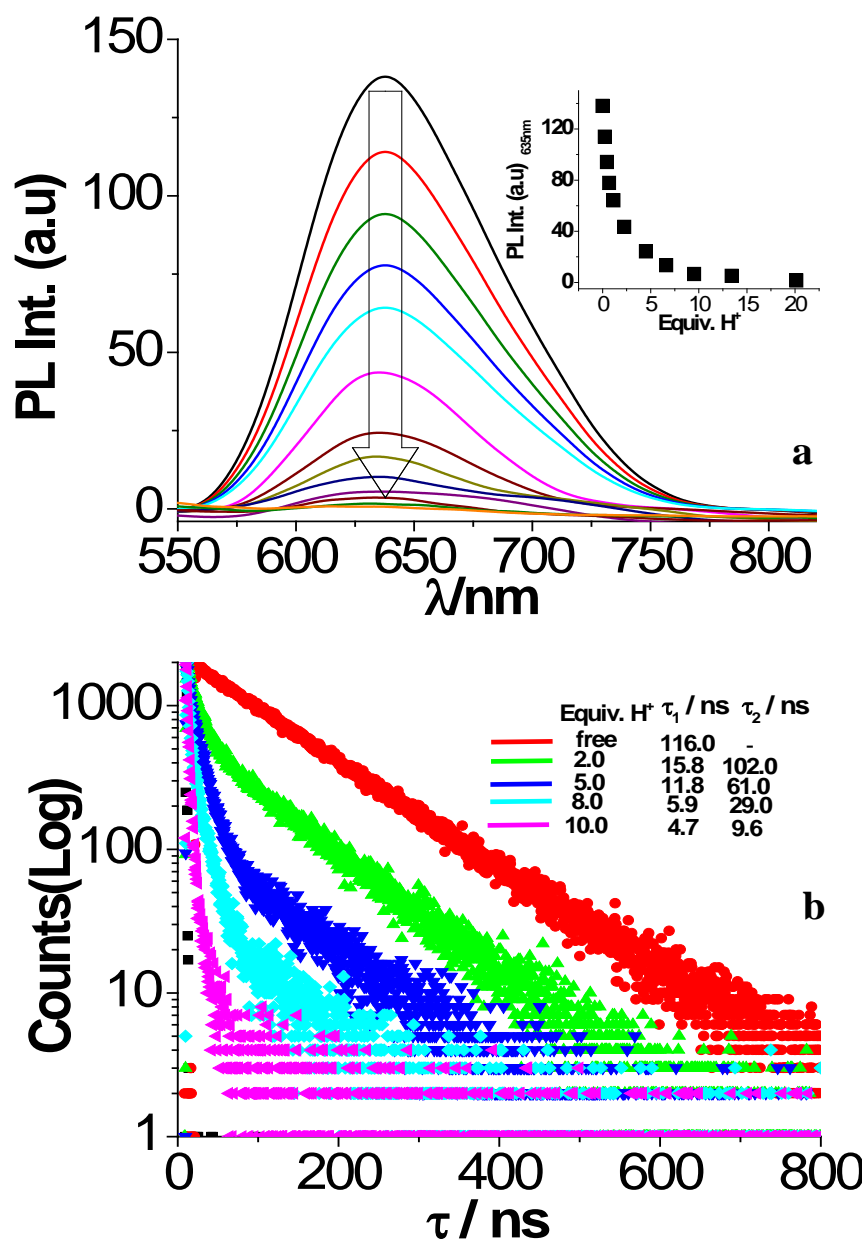


**Fig. S9** Changes in photoluminescence spectra (a) and time-resolved luminescence decay profiles (b) of **1** in acetonitrile at room temperature on incremental addition of  $\text{HClO}_4$ . The inset shows the change of emission intensity (a) and lifetimes (b) of **1** as a function of the equivalent of  $\text{HClO}_4$  added.

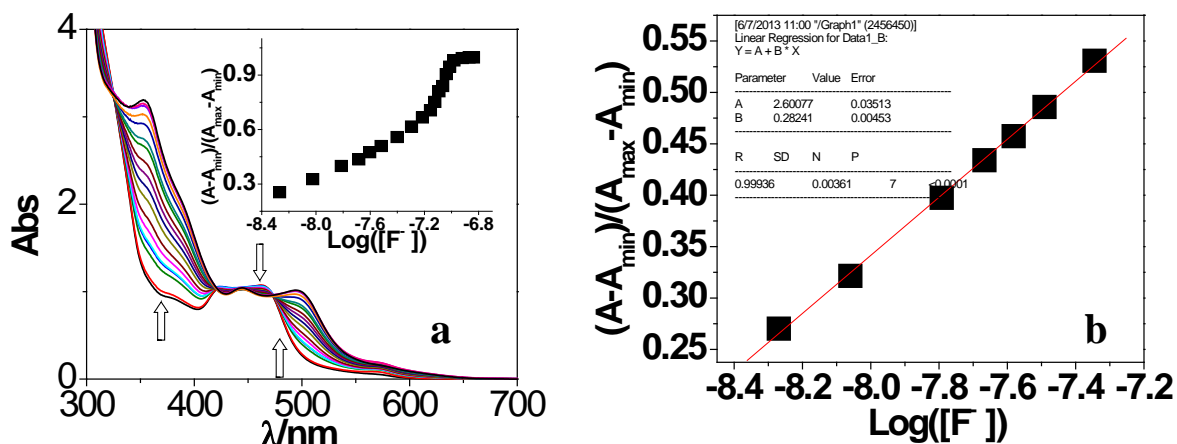


**Fig. S10** (a) Absorbance changes during the titration of **1** ( $2.0 \times 10^{-5}$  M) with  $F^-$  ( $5.0 \times 10^{-3}$  M) in acetonitrile. Normalized absorbance between the minimum absorbance and the maximum absorbance. (b) A plot of  $(A-A_{\min})/(A_{\max}-A_{\min})$  vs  $\text{Log}([F^-])$ , the calculated detection limit of receptor is  $4.34 \times 10^{-9}$  M.

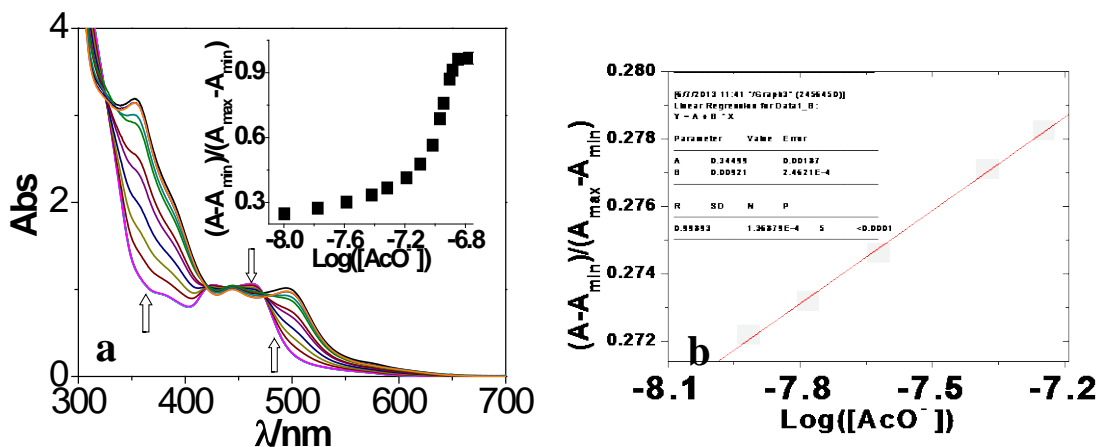


**Fig. S11** (a) Absorbance changes during the titration of **1** ( $2.0 \times 10^{-5}$  M) with  $AcO^-$  ( $5.0 \times 10^{-3}$  M) in acetonitrile. Normalized absorbance between the minimum absorbance and the maximum absorbance. (b) A plot of  $(A-A_{\min})/(A_{\max}-A_{\min})$  vs  $\text{Log}([AcO^-])$ , the calculated detection limit of receptor is  $1.03 \times 10^{-8}$  M.

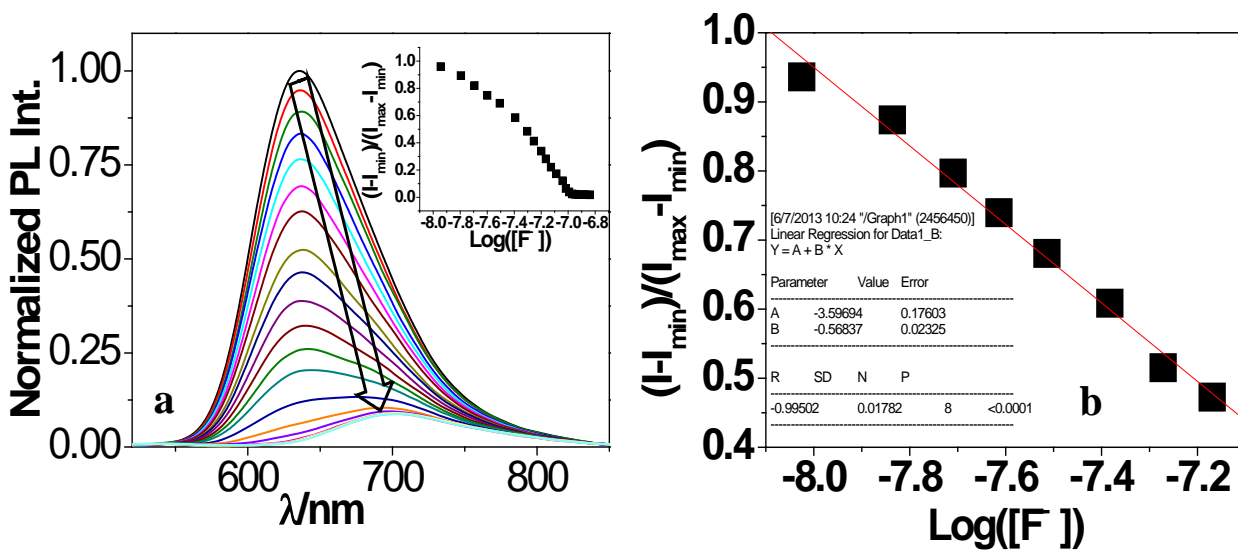


**Fig. S12** (a) Luminescence changes during the titration of **1** ( $2.0 \times 10^{-5}$  M) with  $F^-$  ( $5.0 \times 10^{-3}$  M) in acetonitrile, inset: Normalized intensity between the minimum intensity and the maximum intensity. (b) A plot of  $(I-I_{\min})/(I_{\max}-I_{\min})$  vs  $\text{Log}([F^-])$ , the calculated detection limit of receptor is  $8.19 \times 10^{-9}$  M.

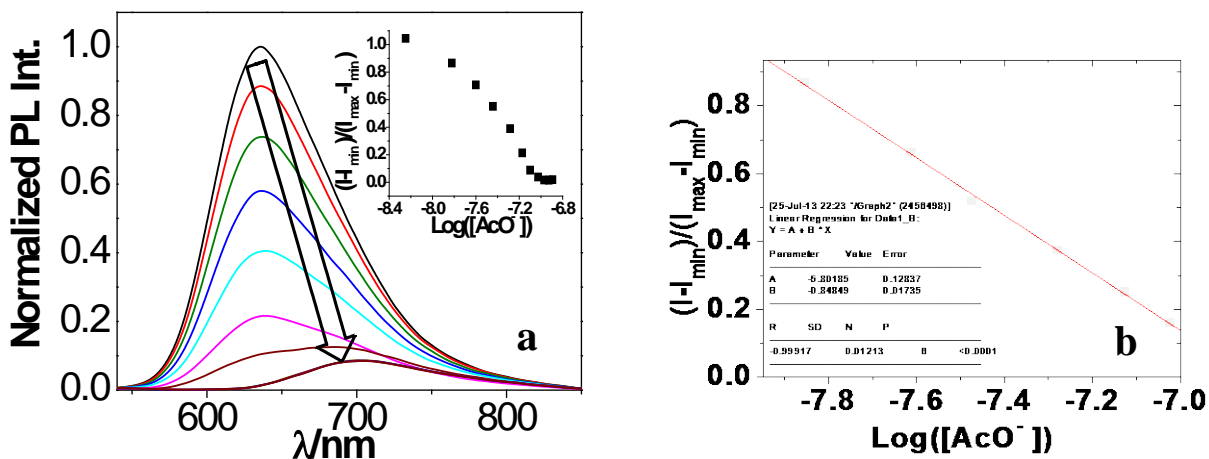


**Fig. S13** (a) Luminescence changes during the titration of **1** ( $2.0 \times 10^{-5}$  M) with  $AcO^-$  ( $5.0 \times 10^{-3}$  M) in acetonitrile, inset: Normalized intensity between the minimum intensity and the maximum intensity. (b) A plot of  $(I-I_{\min})/(I_{\max}-I_{\min})$  vs  $\text{Log}([AcO^-])$ , the calculated detection limit of receptor is  $1.19 \times 10^{-8}$  M.

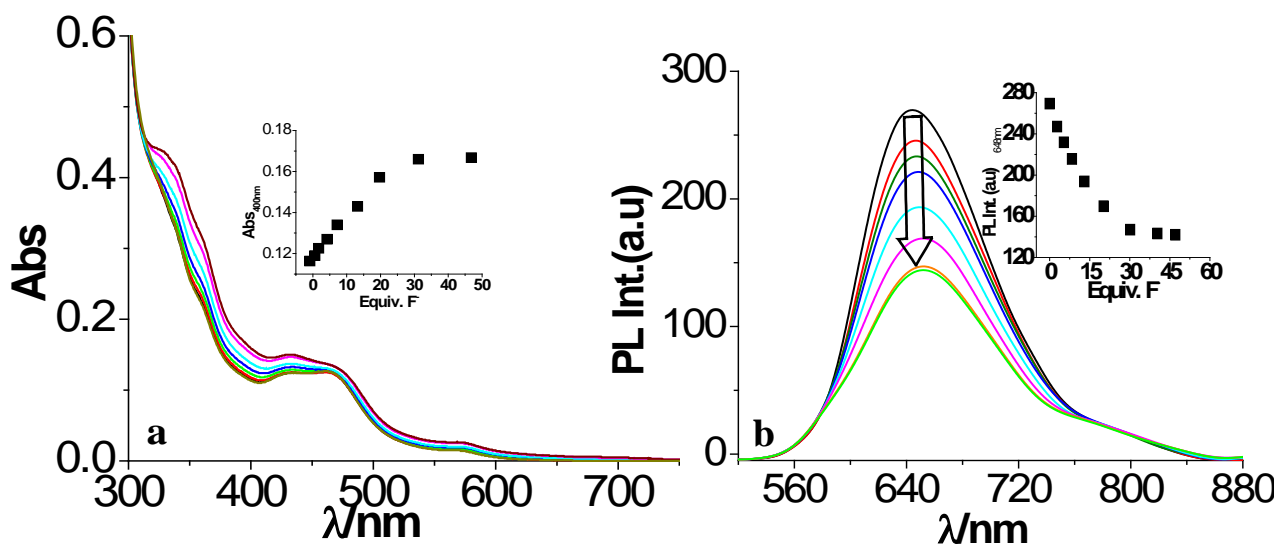


**Fig. S14** Changes in UV-vis absorption (a) and photoluminescence spectra (b) of **1** in water upon addition of  $F^-$  ion.

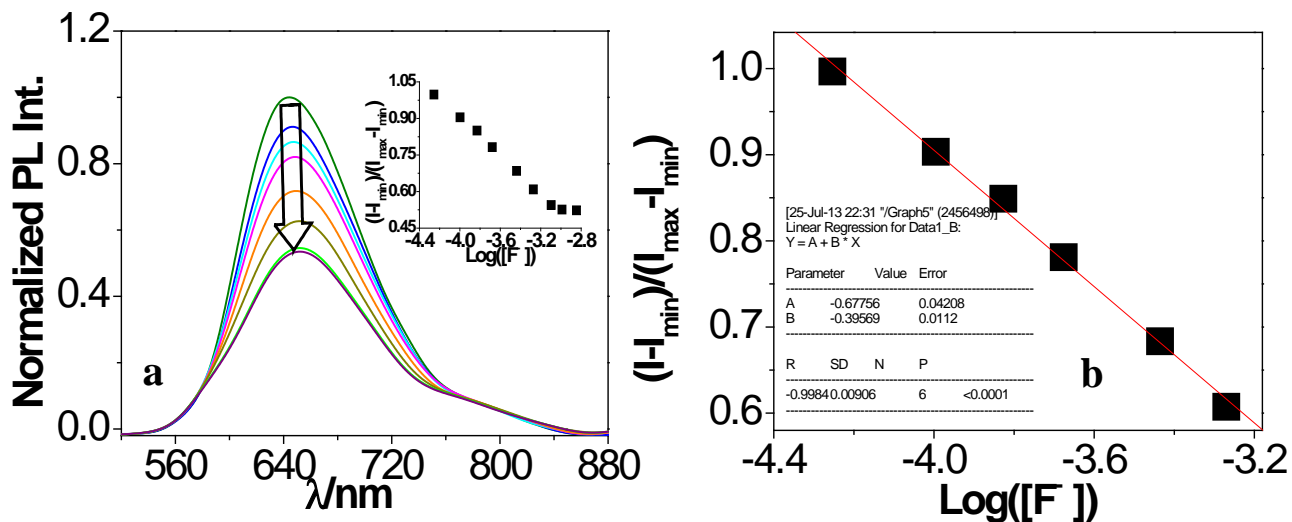


**Fig. S15** (a) Luminescence changes during the titration of **1** ( $2.0 \times 10^{-5}$  M) with  $F^-$  ( $5.0 \times 10^{-3}$  M) in water, inset: Normalized intensity between the minimum intensity and the maximum intensity. (b) A plot of  $(I-I_{\min})/(I_{\max}-I_{\min})$  vs  $\text{Log}([F^-])$ , the calculated detection limit of receptor is  $4.75 \times 10^{-5}$  M.

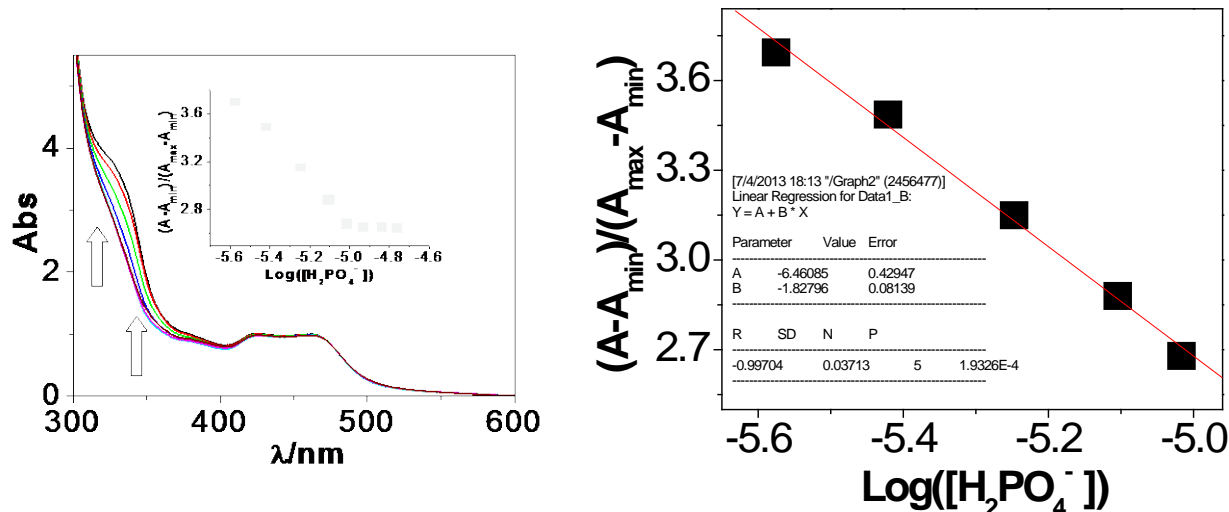


**Fig. S16** (a) Absorbance changes during the titration of **1** ( $2.0 \times 10^{-5}$  M) with  $\text{H}_2\text{PO}_4^-$  ( $5.0 \times 10^{-3}$  M) in acetonitrile. Normalized absorbance between the minimum absorbance and the maximum absorbance. (b) A plot of  $(A-A_{\min})/(A_{\max}-A_{\min})$  vs  $\text{Log}([\text{H}_2\text{PO}_4^-])$ , the calculated detection limit of receptor is  $2.30 \times 10^{-6}$  M.

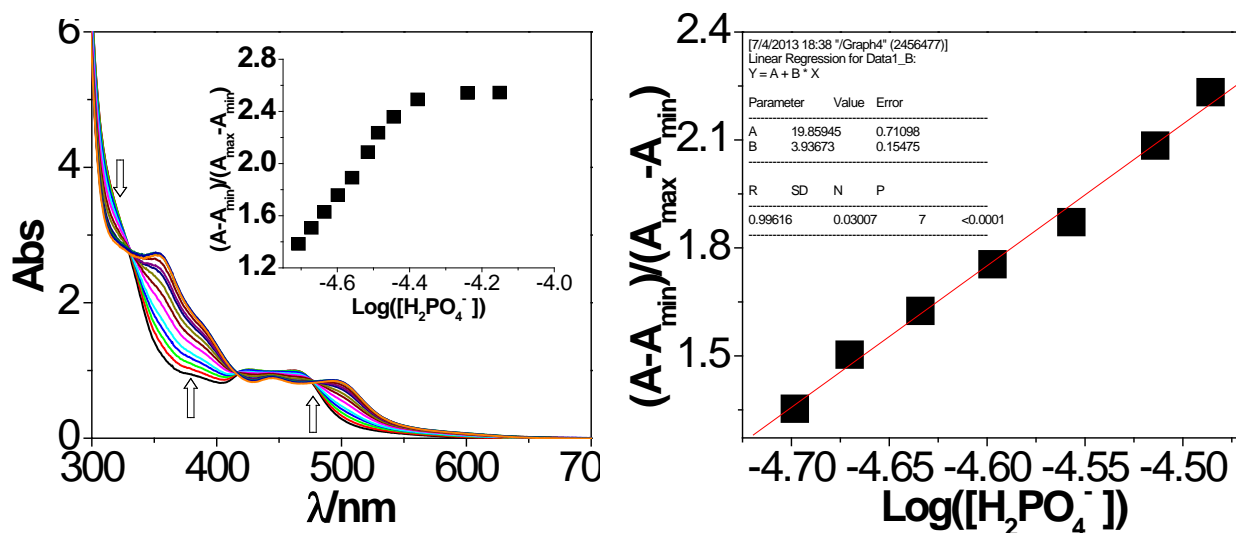


**Fig. S17** (a) Absorbance changes during the titration of **1** ( $2.0 \times 10^{-5}$  M) with  $\text{H}_2\text{PO}_4^-$  ( $5.0 \times 10^{-3}$  M) in acetonitrile. Normalized absorbance between the minimum absorbance and the maximum absorbance. (b) A plot of  $(A-A_{\min})/(A_{\max}-A_{\min})$  vs  $\text{Log}([\text{H}_2\text{PO}_4^-])$ , the calculated detection limit of receptor is  $1.89 \times 10^{-5}$  M.

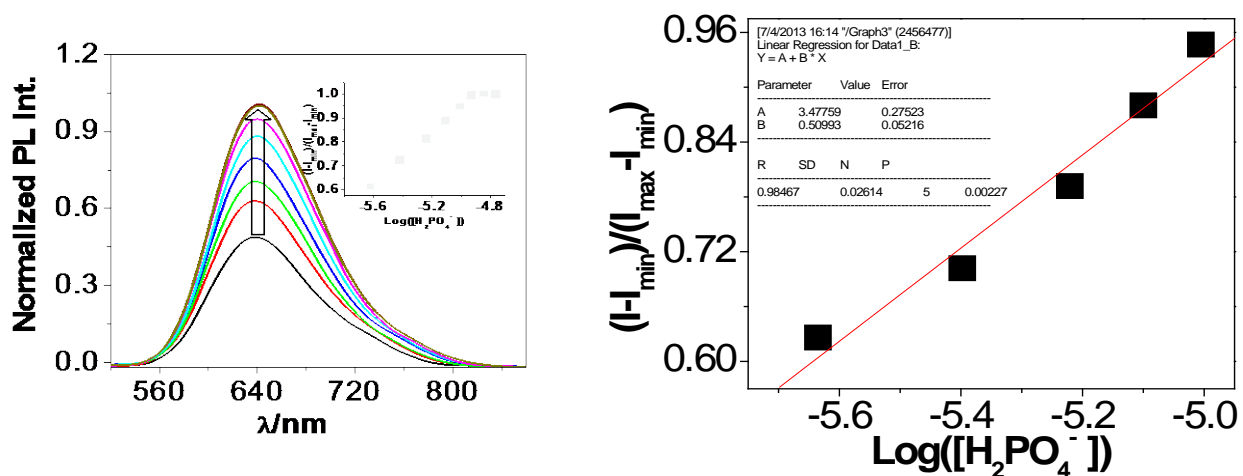


**Fig. S18** (a) Luminescence changes during the titration of **1** ( $2.0 \times 10^{-5}$  M) with  $\text{H}_2\text{PO}_4^-$  ( $5.0 \times 10^{-3}$  M) in acetonitrile, inset: normalized intensity between the minimum intensity and the maximum intensity. (b) A plot of  $(I-I_{\min})/(I_{\max}-I_{\min})$  vs  $\text{Log}([\text{H}_2\text{PO}_4^-])$ , the calculated detection limit of receptor is  $1.99 \times 10^{-6}$  M.

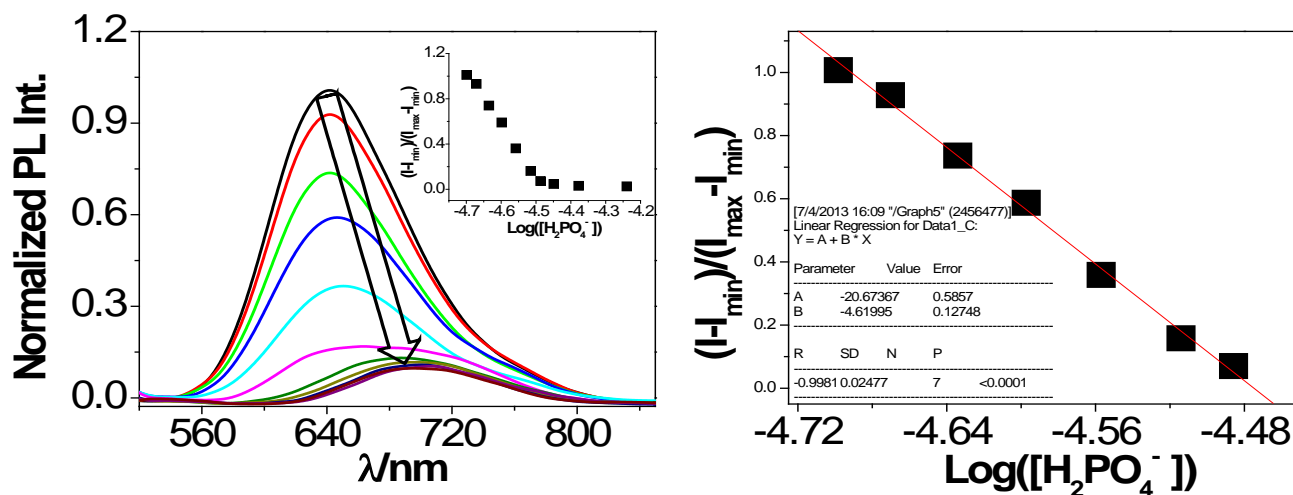


**Fig. S19** (a) Luminescence changes during the titration of **1** ( $2.0 \times 10^{-5}$  M) with  $\text{H}_2\text{PO}_4^-$  ( $5.0 \times 10^{-3}$  M) in acetonitrile, inset: normalized intensity between the minimum intensity and the maximum intensity. (b) A plot of  $(I-I_{\min})/(I_{\max}-I_{\min})$  vs  $\text{Log}([\text{H}_2\text{PO}_4^-])$ , the calculated detection limit of receptor is  $1.90 \times 10^{-5}$  M.

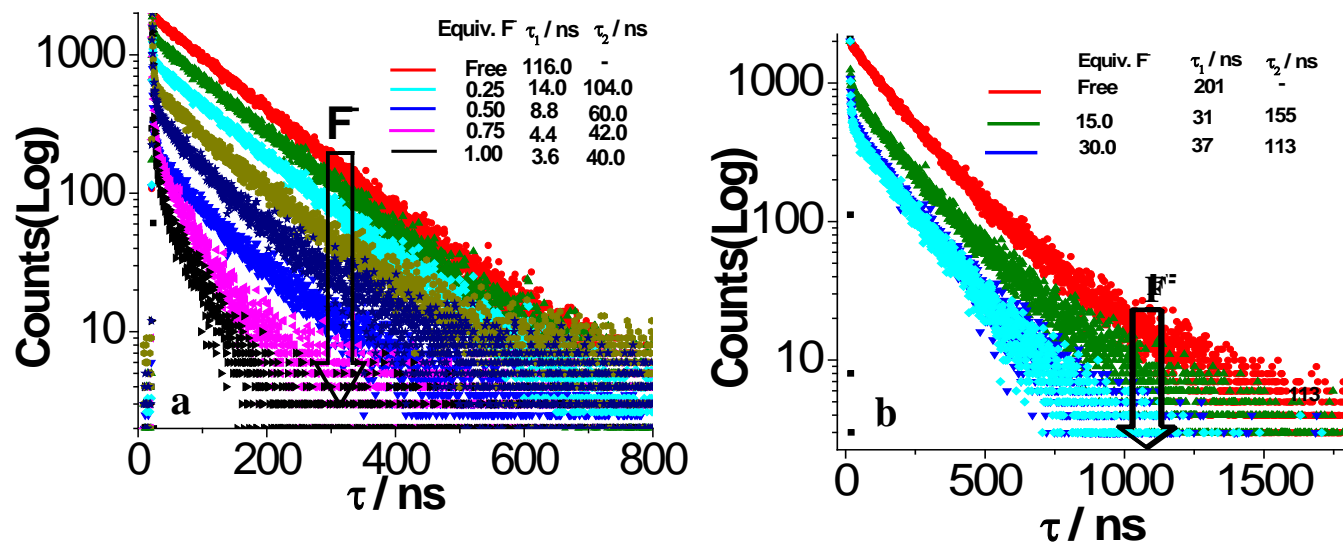


**Fig. S20** Changes in time resolved luminescence decay profiles of **1** upon addition of F<sup>-</sup> in its acetonitrile (a) and aqueous (b) solution. Lifetimes values are also given in the inset of the figure.

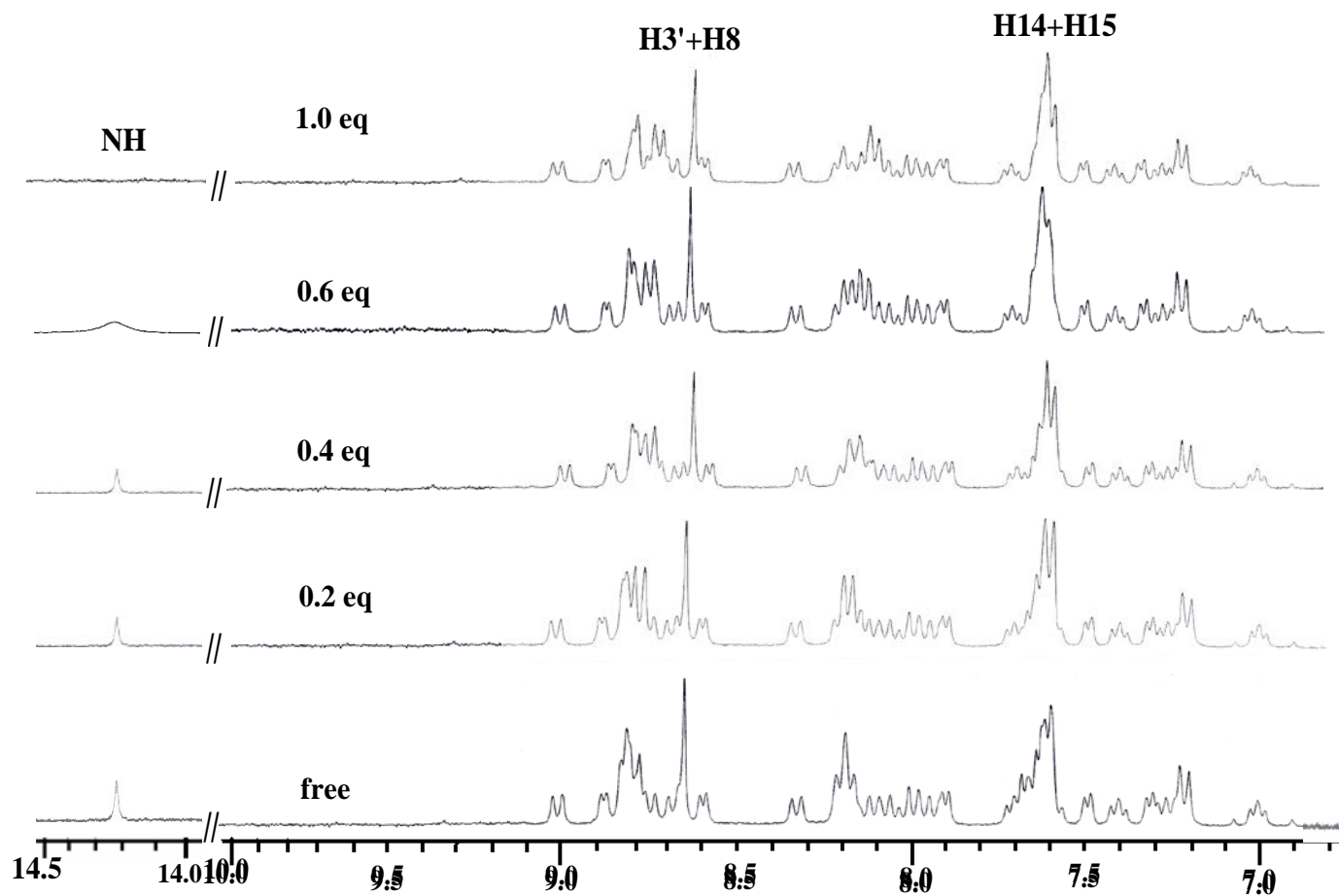


**Fig. S21**  $^1\text{H}$  NMR titration of **1** in  $\text{DMSO-}d_6$  solution ( $5.0 \times 10^{-3}$  M) upon addition of  $\text{F}^-$  ion ( $1.25 \times 10^{-1}$  M, 0–1 equiv).

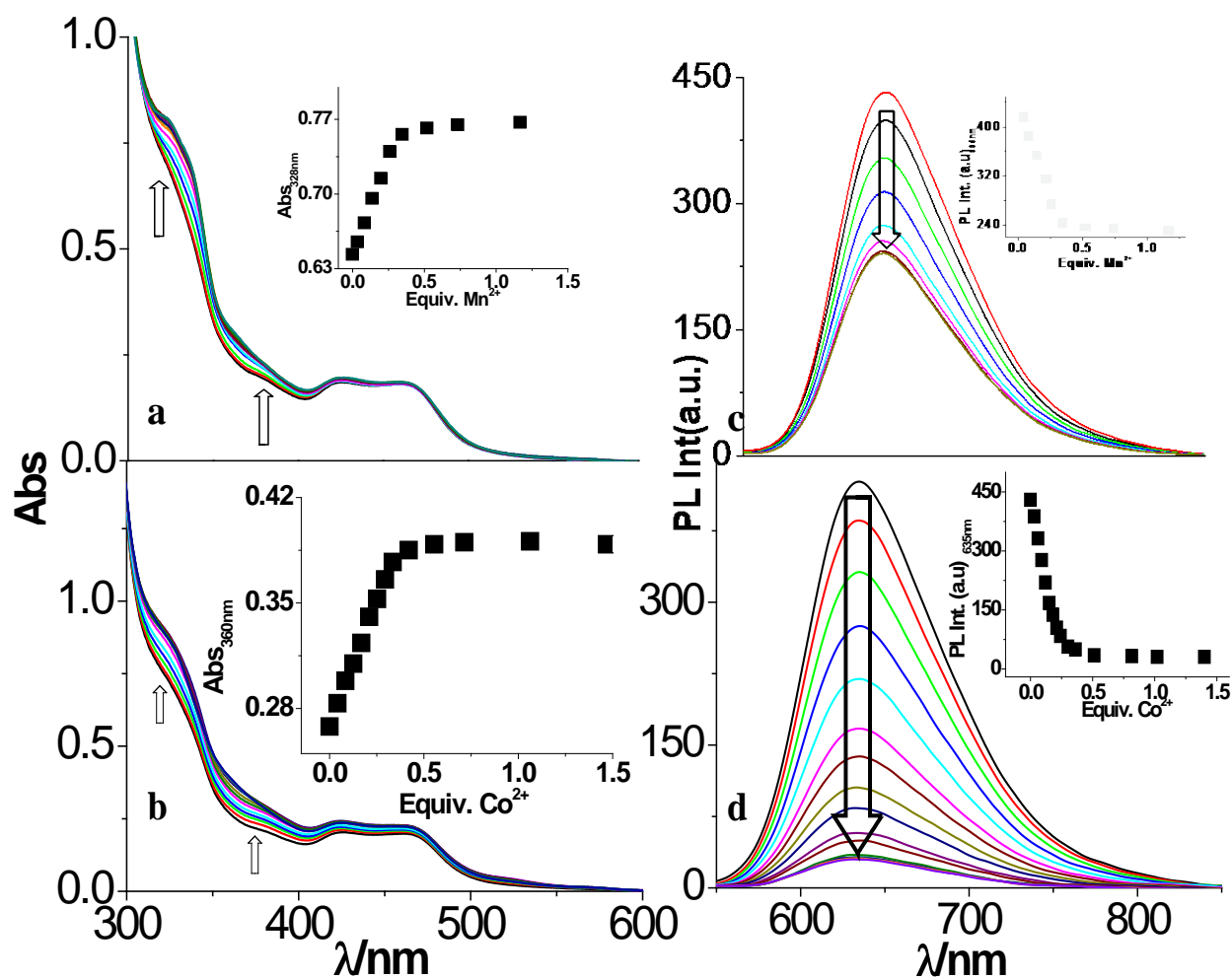


**Fig. S22** Changes in UV-vis and photoluminescence spectra of **1** in acetonitrile upon addition of Mn(ClO<sub>4</sub>)<sub>2</sub> (a and c, respectively) and Co(ClO<sub>4</sub>)<sub>2</sub> (b and d, respectively). The inset shows the change of absorption and emission intensity as a function of the equivalent of Mn<sup>2+</sup> and Co<sup>2+</sup> ions added.

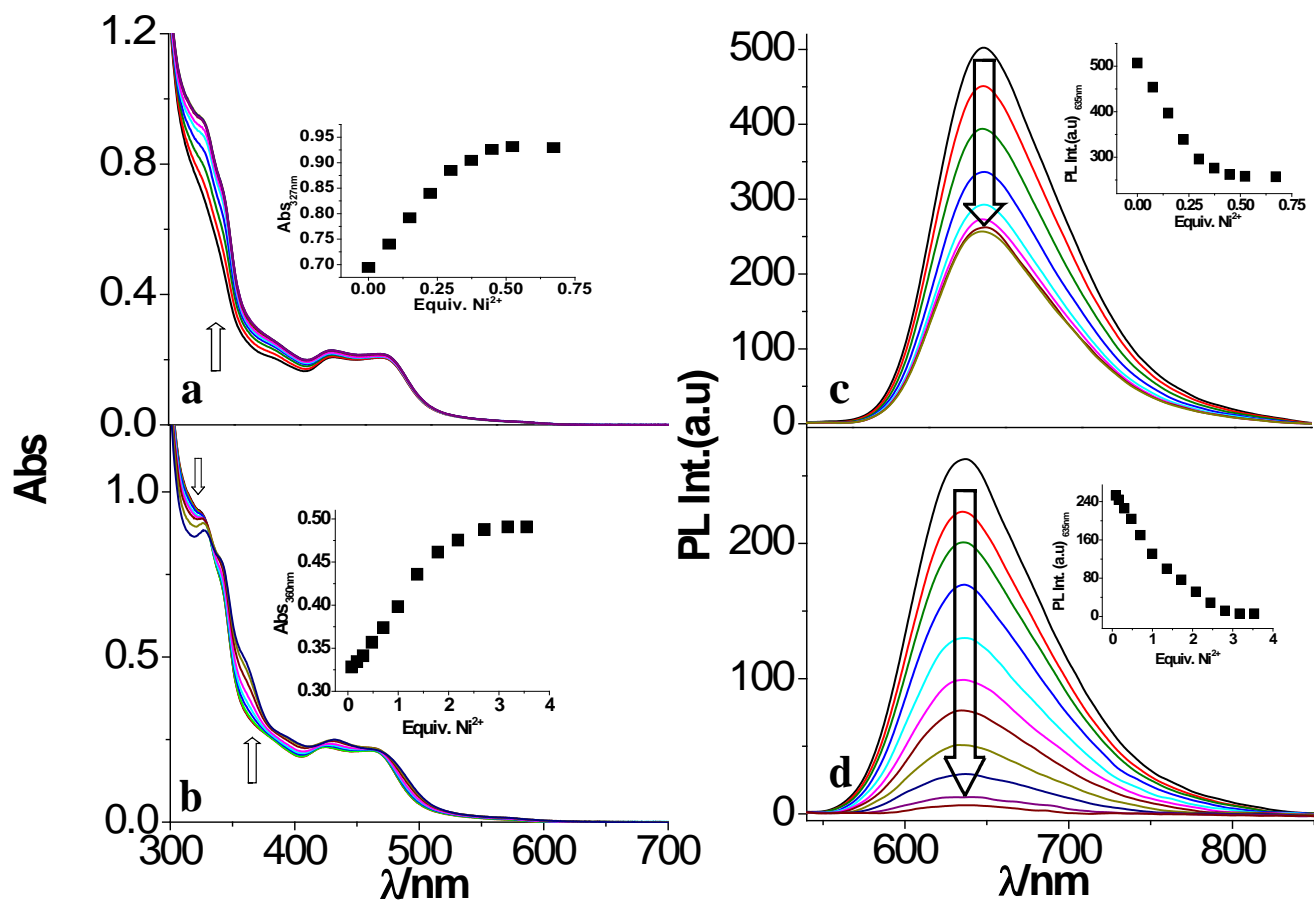


**Fig. 23** Changes in UV-vis absorption (a and b) and photoluminescence spectra (c and d) of **1** in acetonitrile upon incremental addition of  $\text{Ni}(\text{ClO}_4)_2$ . The inset shows the change of absorption and emission intensity as a function of the equivalent of  $\text{Ni}^{2+}$  ion added.

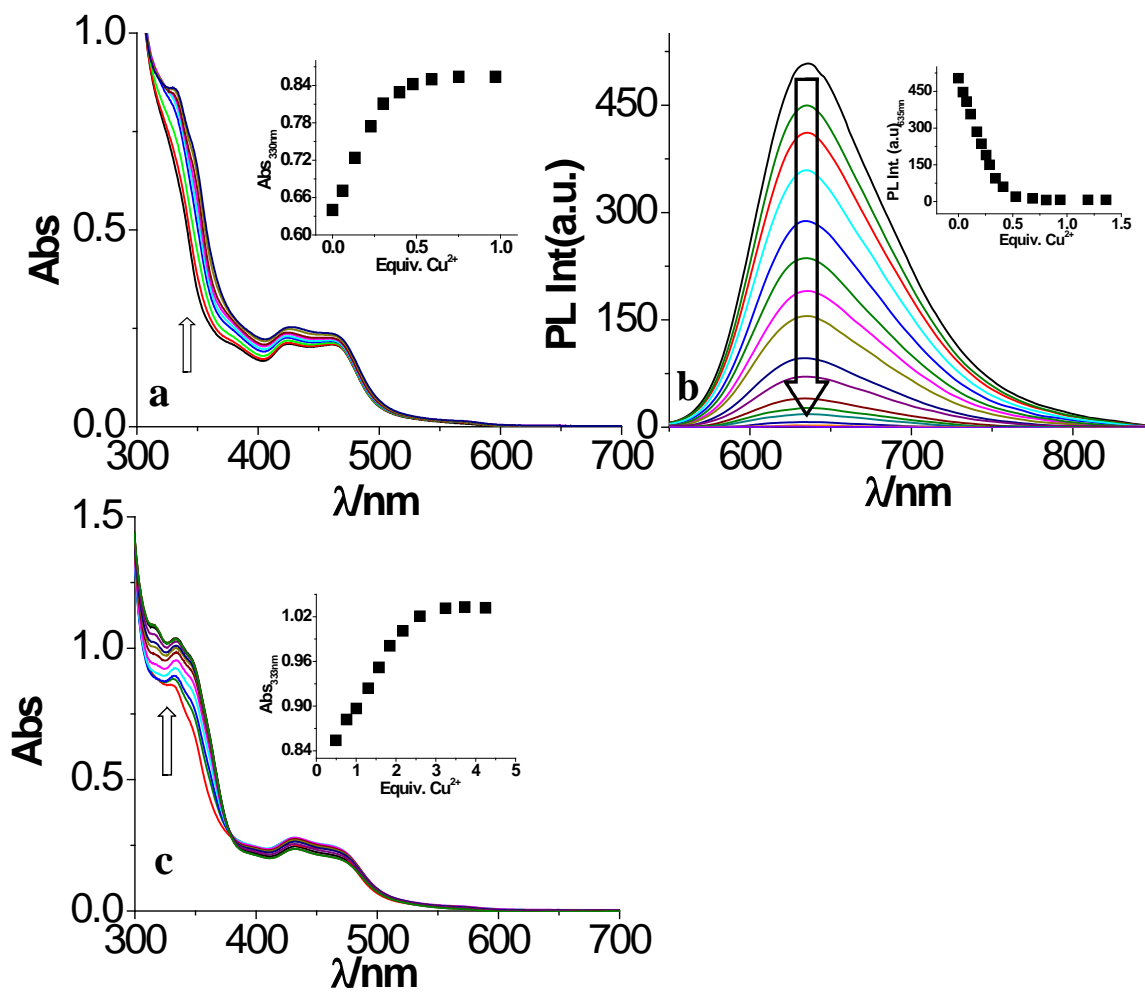


**Fig. S24** Changes in UV-vis absorption (a and c) and photoluminescence spectra (b) of **1** in acetonitrile upon addition of  $\text{Cu}(\text{ClO}_4)_2$ . The inset shows the change of absorption and emission intensity as a function of the equivalent of  $\text{Cu}^{2+}$  ion added.

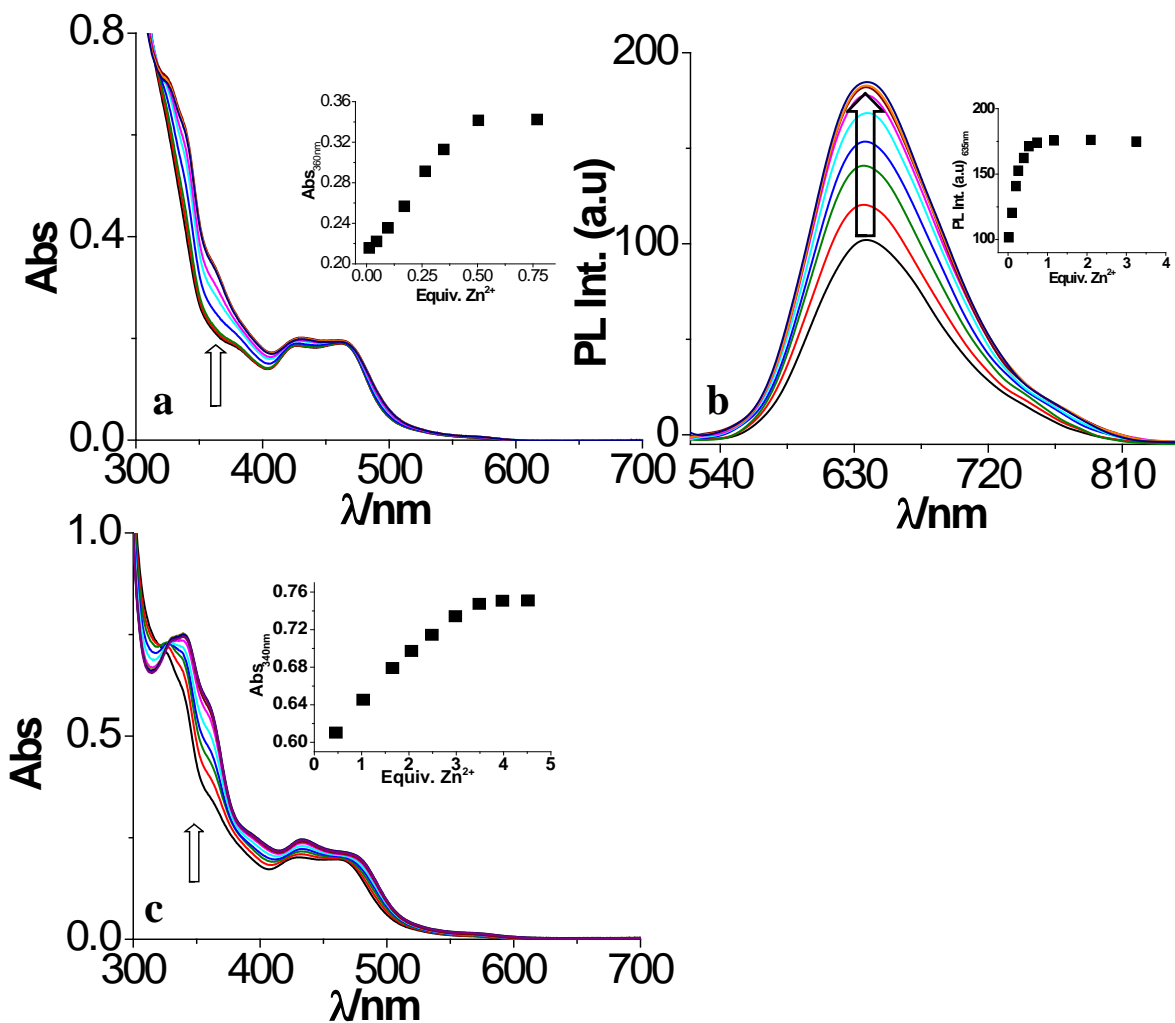


**Fig. S25** Changes in UV-vis absorption (a and c) and photoluminescence (b) spectra of **1** in acetonitrile upon addition of  $\text{Zn}(\text{ClO}_4)_2$ . The inset shows the change of absorption and emission intensity as a function of the equivalent of  $\text{Zn}^{2+}$  ion added.

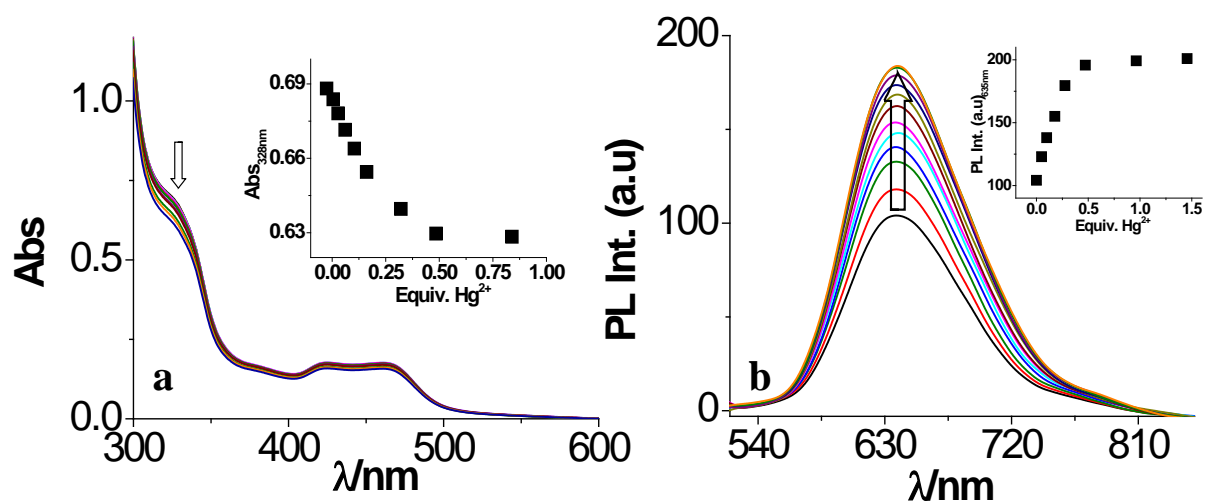


**Fig. S26** Changes in UV-vis absorption (a) and photoluminescence (b) spectra of **1** in acetonitrile upon addition of  $\text{Hg}(\text{ClO}_4)_2$ . The inset shows the change of absorption and emission intensity as a function of the equivalent of  $\text{Hg}^{2+}$  ion added.

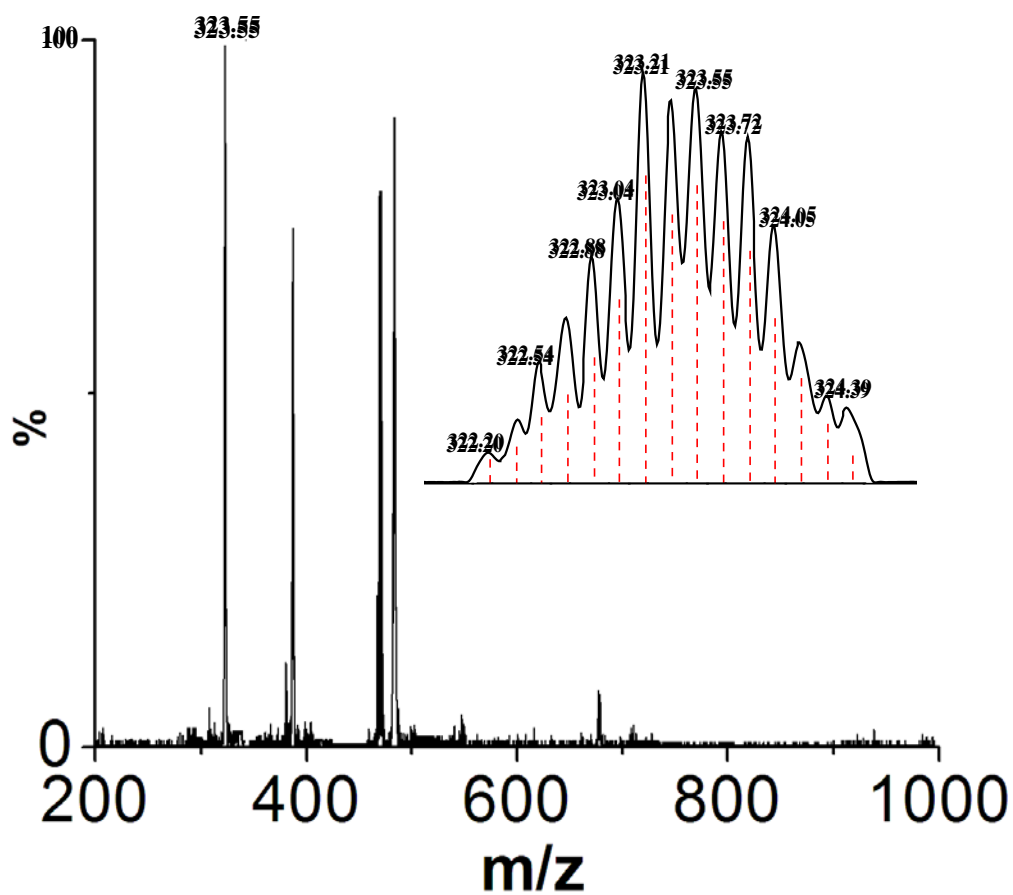


**Fig. S27** Experimental ESI mass spectra (positive) for **1** in acetonitrile in the presence Fe<sup>2+</sup>. Inset shows the observed and simulated isotopic distribution patterns of the peak at m/z = 323.55.

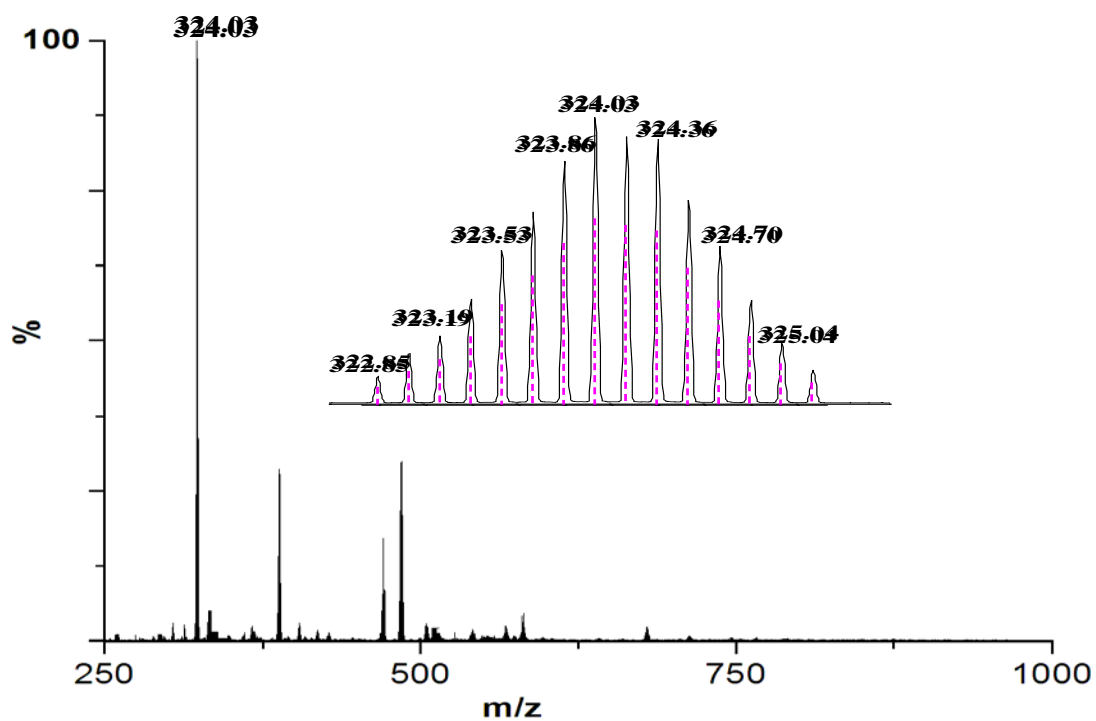


**Fig. S28** Experimental ESI mass spectra (positive) for **1** in acetonitrile in the presence  $\text{Ni}^{2+}$ . Inset shows the observed and simulated isotopic distribution patterns of the peak at  $m/z = 324.03$ .

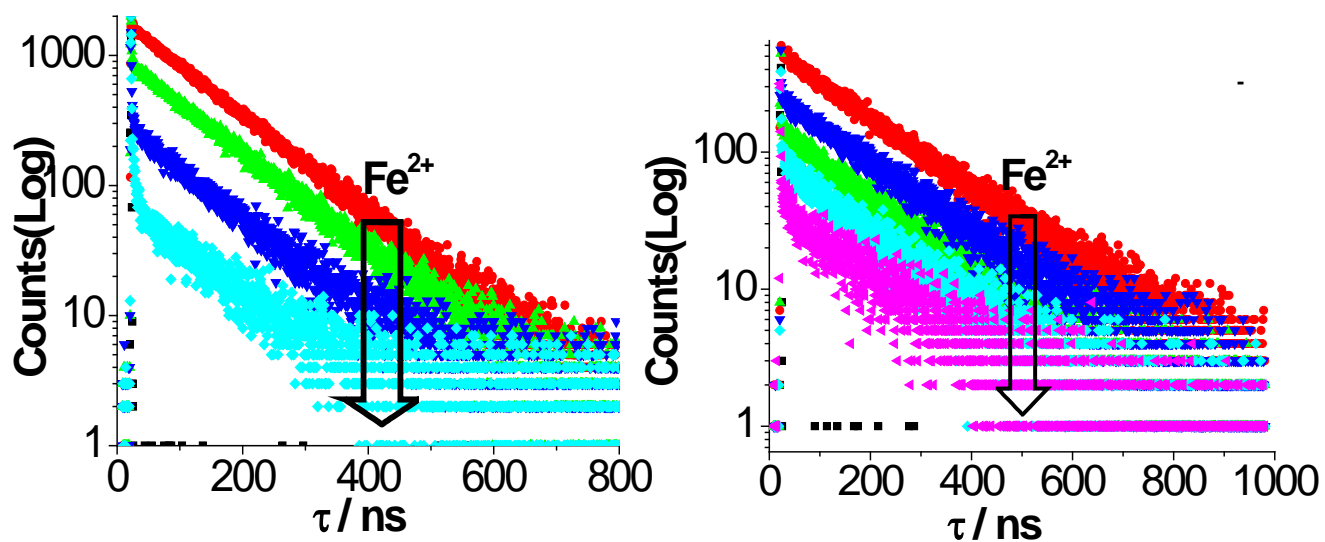


**Fig. S29** Changes in time resolved luminescence decay profiles of **1** upon addition of  $\text{Fe}^{2+}$  ion in its acetonitrile (a) and aqueous (b) solution.

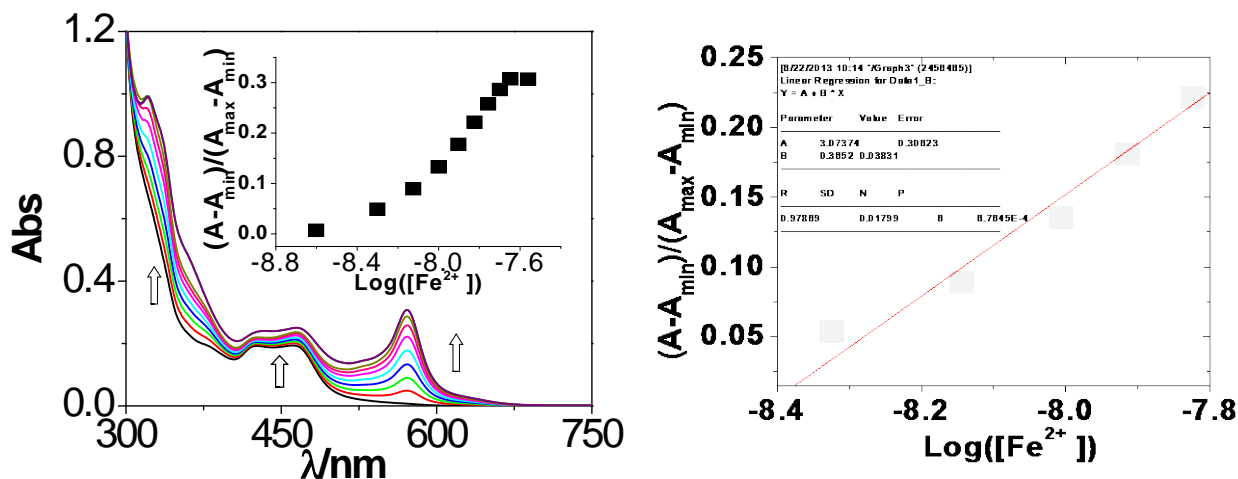


**Fig. S30** (a) Absorbance changes during the titration of **1** ( $2.0 \times 10^{-5}$  M) with  $\text{Fe}^{2+}$  ( $5.0 \times 10^{-3}$  M) in acetonitrile. Normalized absorbance between the minimum absorbance and the maximum absorbance. (b) A plot of  $(A-A_{\min})/(A_{\max}-A_{\min})$  vs  $\text{Log}([\text{Fe}^{2+}])$ , the calculated detection limit of receptor is  $6.68 \times 10^{-9}$  M.

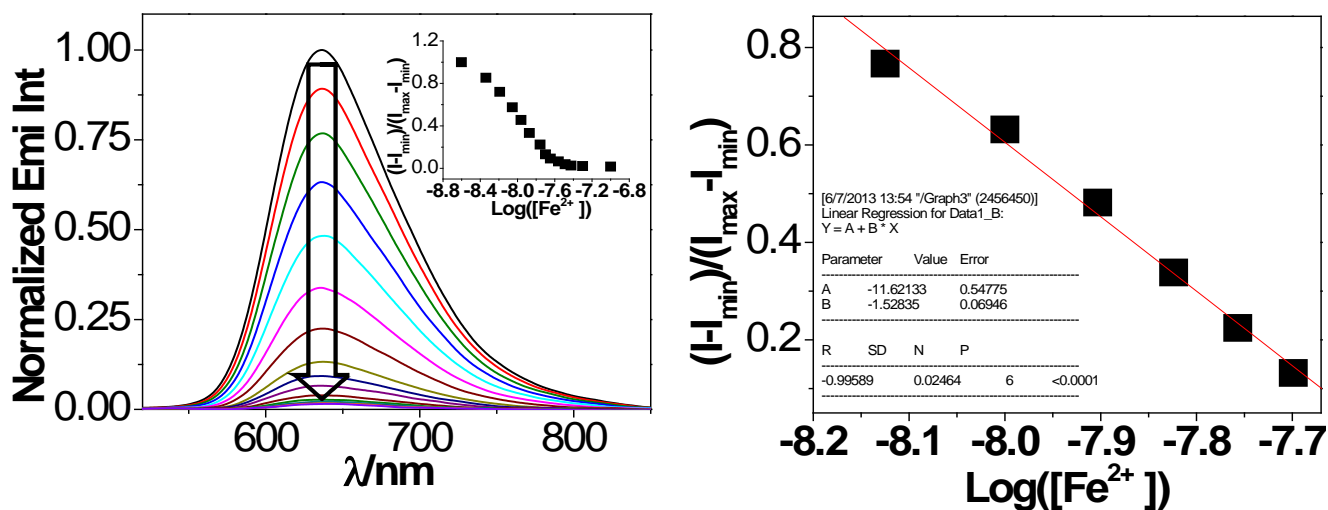


**Fig. S31** (a) Luminescence changes during the titration of **1** ( $2.0 \times 10^{-5}$  M) with  $\text{Fe}^{2+}$  ( $5.0 \times 10^{-3}$  M) in acetonitrile, inset: normalized intensity between the minimum intensity and the maximum intensity. (b) A plot of  $(I-I_{\min})/(I_{\max}-I_{\min})$  vs  $\text{Log}([\text{Fe}^{2+}])$ , the calculated detection limit of receptor is  $6.78 \times 10^{-9}$  M.

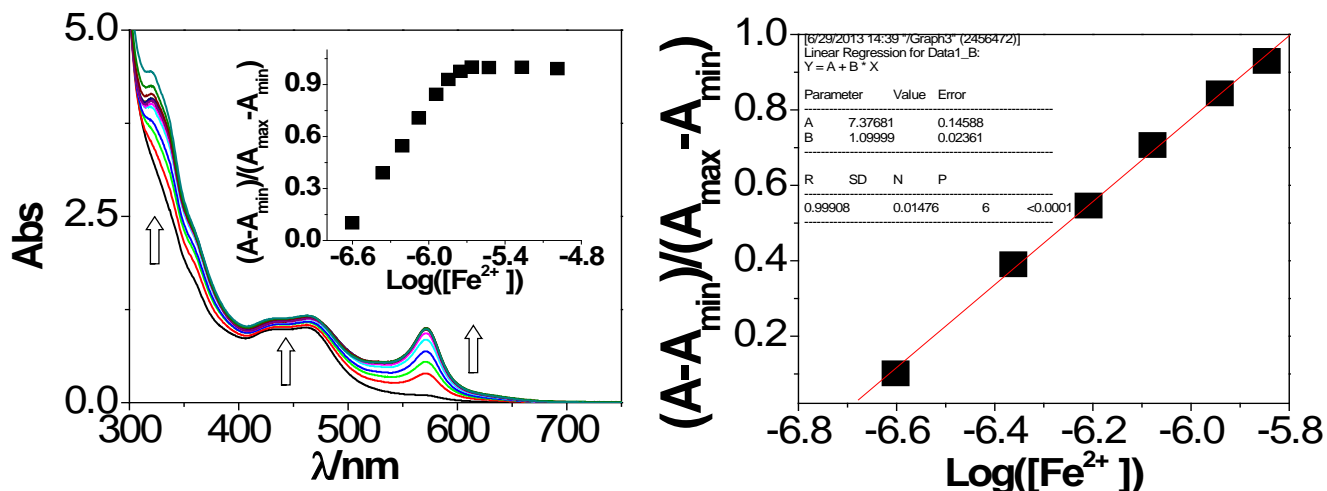


**Fig. S32** (a) Absorbance changes during the titration of **1** ( $2.0 \times 10^{-5}$  M) with  $\text{Fe}^{2+}$  ( $5.0 \times 10^{-3}$  M) in water. Normalized absorbance between the minimum absorbance and the maximum absorbance. (b) A plot of  $(A-A_{\min})/(A_{\max}-A_{\min})$  vs  $\text{Log}([\text{Fe}^{2+}])$ , the calculated detection limit of receptor is  $2.18 \times 10^{-7}$  M.

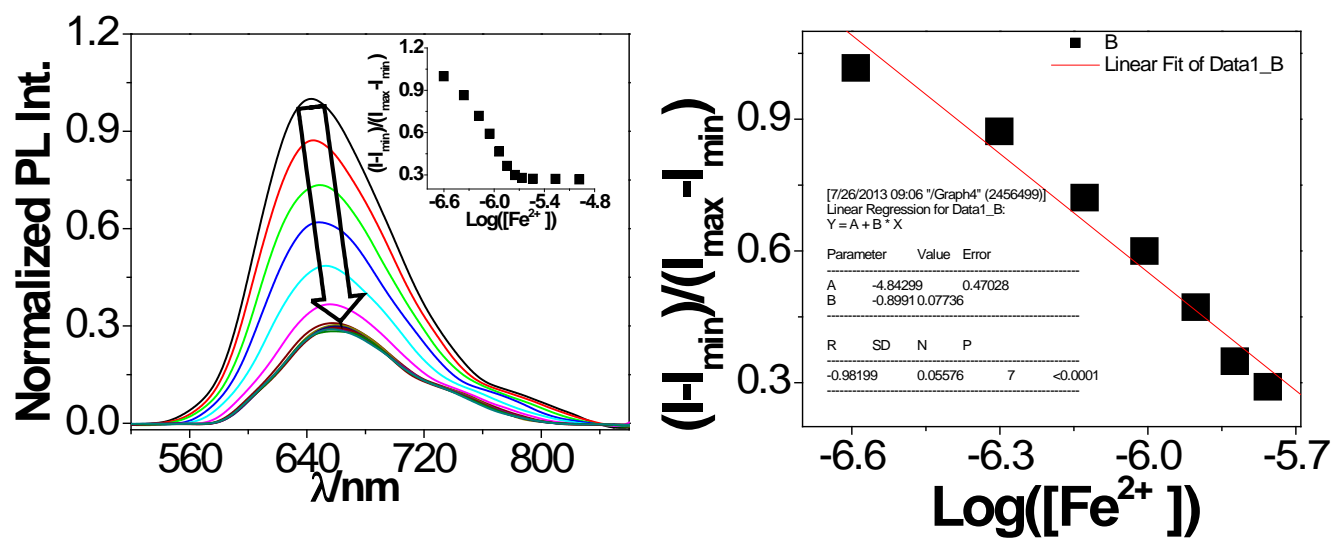


**Fig. S33** (a) Luminescence changes during the titration of **1** ( $2.0 \times 10^{-5}$  M) with  $\text{Fe}^{2+}$  ( $5.0 \times 10^{-3}$  M) in water, inset: normalized intensity between the minimum intensity and the maximum intensity. (b) A plot of  $(I-I_{\min})/(I_{\max}-I_{\min})$  vs  $\text{Log}([\text{Fe}^{2+}])$ , the calculated detection limit of receptor is  $2.38 \times 10^{-7}$  M.

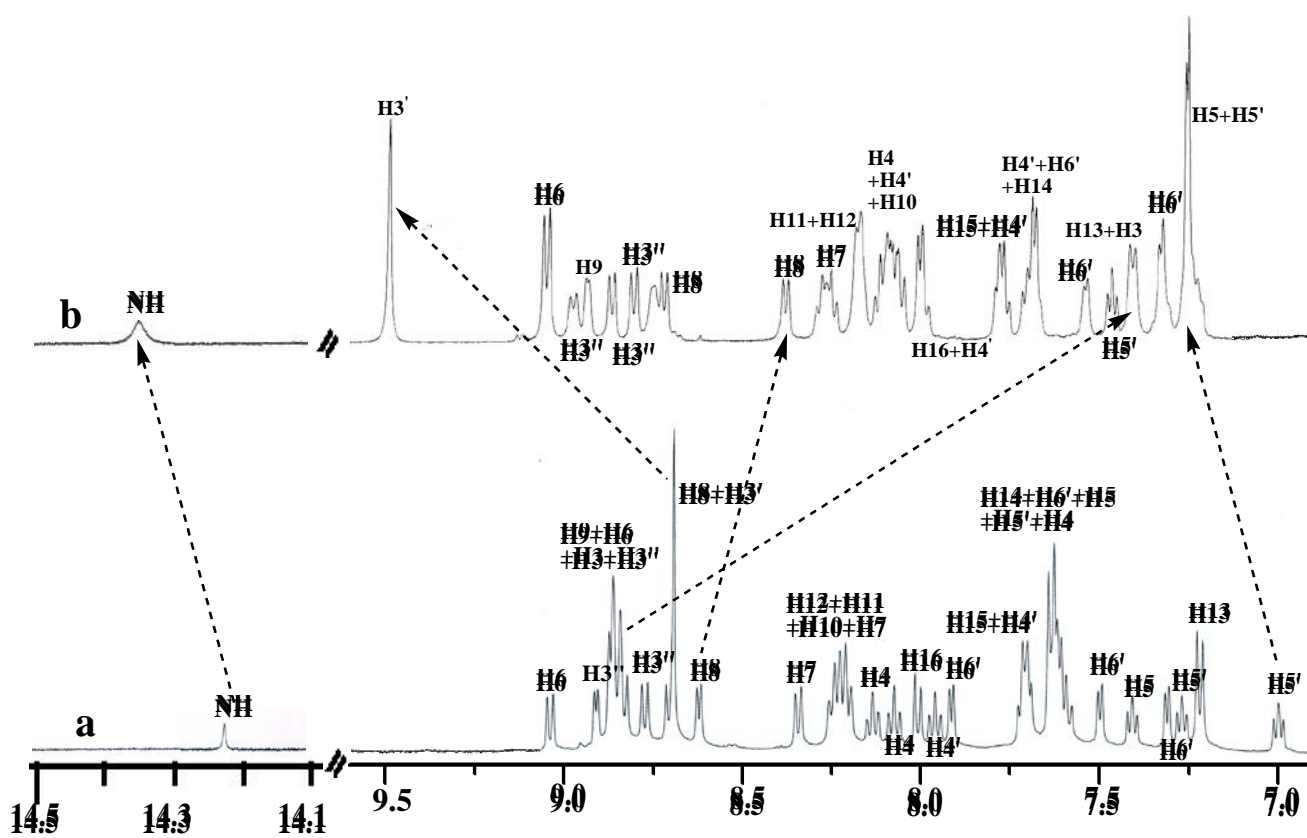


**Fig. S34** <sup>1</sup>H NMR spectra of **1** in DMSO-*d*<sub>6</sub> ( $5.0 \times 10^{-3}$  M) in absence (a) and in presence of 0.5 equiv. of Fe<sup>2+</sup> ion (b).

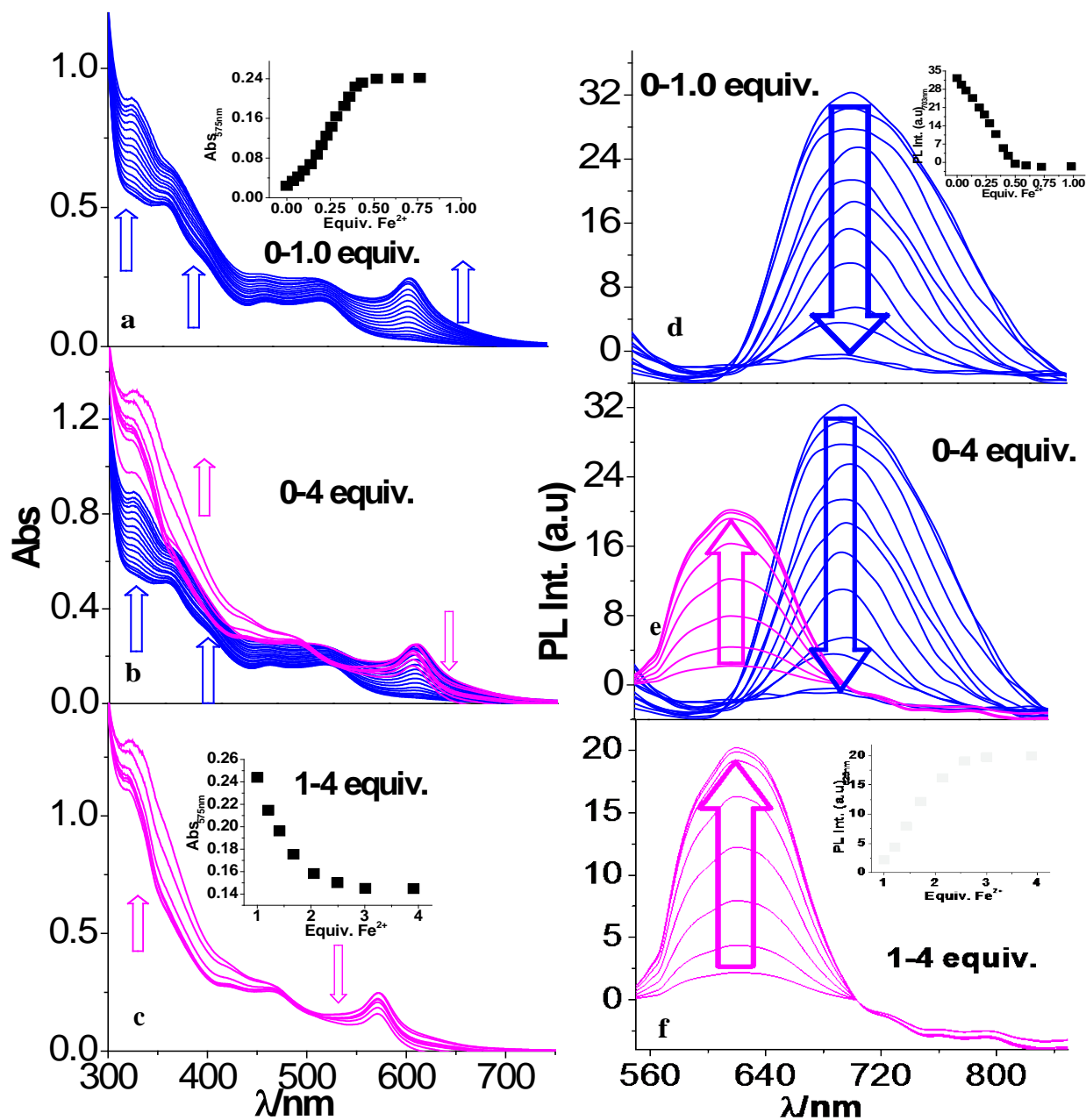


**Fig. S35** Changes in UV-vis absorption (a-c) and photoluminescence (d-f) spectra of **1** in acetonitrile upon incremental addition of  $\text{Fe}^{2+}$  in the presence of 1 equiv. of  $\text{F}^-$  ion.

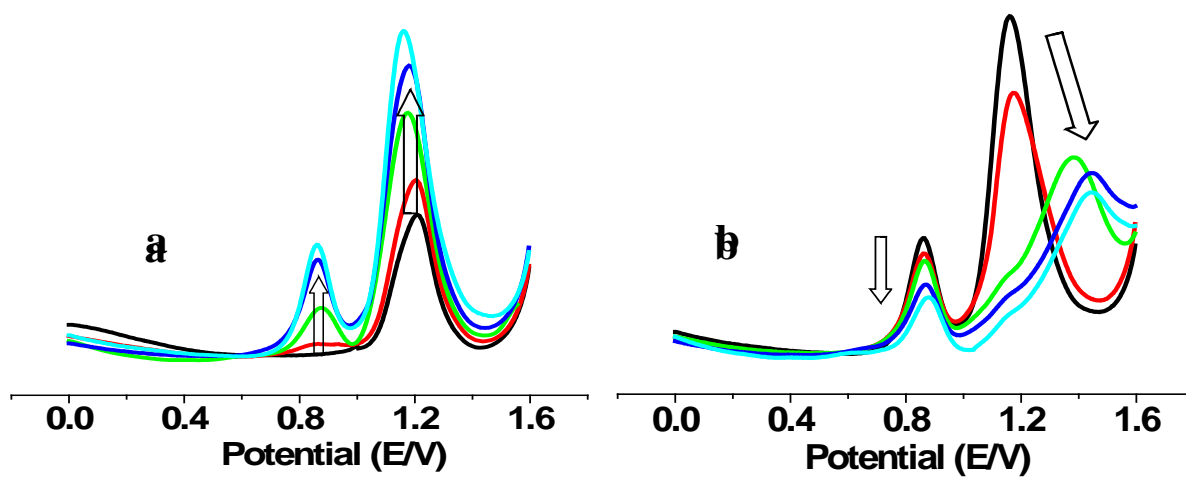


**Fig. S36** Changes of SWVs of **1** on incremental addition of  $F^-$  (a: 0-2 equiv. and b: 2-10 equiv.) in the presence of 0.5 equiv. of  $Fe^{2+}$  ion.

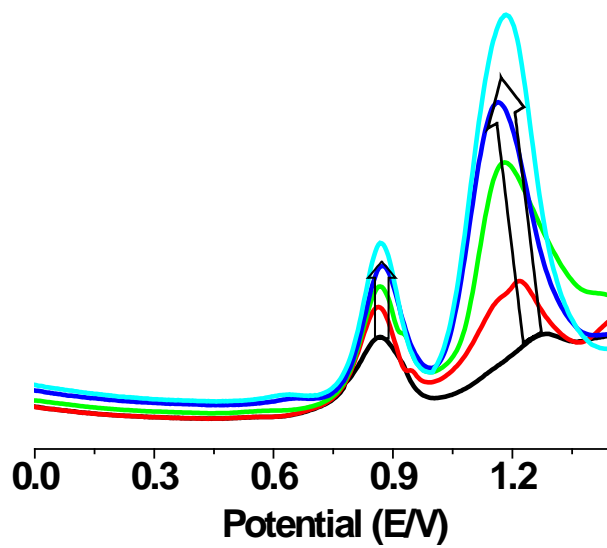


**Fig. S37** Changes of SWVs of **1** on incremental addition of Fe<sup>2+</sup> (0-1 equiv.) in the presence of 1.0 equiv of F<sup>-</sup> ion.